Electronic structure of the ion pair model for Ti:Al_2O_3

1994 J. Phys.: Condens. Matter 6 6497

(http://iopscience.iop.org/0953-8984/6/32/011)

J. Phys.: Condens. Matter 6 (1994) 6497–6505. Printed in the UK

Electronic structure of the ion pair model for Ti:Al_2O_3

F X Zha†‡, J H Zhang‡ and S D Xia†

† Physics Department, University of Science and Technology of China, Hefei, Anhui 230026, People's Republic of China

‡ Shanghai Institute of Metallurgy, Chinese Academy of Sciences, 865 Changning Road, Shanghai 200050, People's Republic of China

Received 11 October 1993, in final form 28 April 1994

Abstract. The Ti^{3+}–Ti^{4+} ion pair is proposed experimentally to be responsible for the infrared residual absorption of Ti:Al_2O_3. However, no theoretical verification has been presented to date. In this paper, the DV-X_α calculation is performed upon clusters of $(Ti^{3+}O_6^{2-})^{9-}$, $(Ti^{3+}Al^{3+}O_9^{2-})^{12-}$ and $(Ti^{3+}Ti^{4+}O_9^{2-})^{11-}$. Our work not only has interpreted the infrared residual absorption but also has clarified the confusion about the origin of the ultraviolet absorptions. Therefore the Ti^{3+}–Ti^{4+} pair postulation is strongly supported by our present work.

1. Introduction

In recent years, the Ti^{3+}-doped tunable laser crystal has attracted much attention because of its superior characteristics of a large gain cross section, a broad tuning range and the absence of excited absorption. In particular for Ti:Al_2O_3, much progress has been achieved since its laser characteristics were initially reported by Moulton [1]. However, confusion still exists in understanding its spectral features which are connected with the local electronic structure of titanium in the crystal.

The origin of a weak absorption hump at around 800 nm, called the infrared (IR) residual absorption, has aroused much attention because the hump overlaps the range of the laser's output and its existence will greatly impair the laser's efficiency. Earlier, Lacovara *et al* [2] consider that this absorption is due to the Ti^{3+} ion in defect sites or at sites close to native sites; Powell *et al* [3] on the other hand attribute it to the charge-transfer transition between coupled iron–titanium ion pairs. However, it has recently been suggested by Aggarwal *et al* [4] and Sanchez *et al* [5] that the Ti^{3+}–Ti^{4+} pair is primarily responsible for the IR residual absorption.

Another ambiguity, about which there has not been a definite view until now, is in the mechanism of its ultraviolet (UV) absorptions. Usually, the UV absorption humps of laser crystals are linked with the charge-transfer transitions of the doped transition-metal (TM) ions. However, it is doubted by Moulton [6] whether the 6.9 eV absorption hump of Ti:Al_2O_3 should be assigned to the charge-transfer transition of trivalent titanium as done by Tippens [7]. Additionally, another small absorption hump at approximately 4.5–5.0 eV, is attributed by Tippens [7] to the charge-transfer transition of trivalent iron, but the assignment also provokes many questions [2]. Moreover, according to the excitation spectrum, several fine peaks in the UV region can be distinguished but their origin remains uncertain [2].

In an annealing experiment of the crystal in an atmosphere with different oxygen partial pressures, it is found that the intensities of both the IR residual absorption and the UV

0953-8984/94/326497+09$19.50

absorptions are much influenced by the Ti^{4+} ion content. In spite of the different conjectures on the model related to Ti^{4+} [2,3], it should be noted that the Ti^{3+}–Ti^{4+} pair, which determines the IR residual absorption [4,5], may actually be regarded as a type of model for Ti^{4+}. Then it is natural to enquire whether or not the ion pair mechanism also contributes to the UV absorptions.

Therefore it is significant and essential to make a theoretical calculation to resolve the problem as well as to confirm the Ti^{3+}–Ti^{4+} postulation of IR residual absorption. The cluster model computation by the DV-X_α method has proved to be an effective tool in investigation of the local electronic structure of impurity states (see, e.g., [8,9]). At present, we resort to this technique and try to obtain a complete understanding of the spectral features attributed to the Ti^{3+}–Ti^{4+} ion pair. A description of the method is available elsewhere [10–12] and selection of the model used is explained in the following section.

2. Selection of models and computational parameters

Goodenough [13] has studied cation–cation interactions in several oxides including corundum-type compounds such as Ti_2O_3. Three types of ion pair could be formed by neighbouring cations in the corundum structure as shown in figure 1(*a*):

(i) A–B, the cation–anion–cation interaction;

(ii) A–C, the interaction between the cation-occupied octahedra that share a common edge;

(iii) A–A′, the interaction between the cation-occupied octahedra that share a common face.

Goodenough [13] concludes that only the third type of interaction plays a primary role in Ti_2O_3 because it belongs to a 'strong-type' pair interaction which exhibits the most stable bonding state that introduces no change in lattice symmetry. Enlightened by this result, it could be inferred that the type of pair structure existing for Ti^{3+}–Ti^{3+} may also occur for the Ti^{3+}–Ti^{4+} pair in $Ti:Al_2O_3$. This analogy should be reasonable in view of the structural chemistry and the dynamics of crystal growth. Since $Ti:Al_2O_3$ is grown by doping Ti_2O_3 and since Ti_2O_3 possesses the same corundum structure, the pair structure of Ti^{3+}–Ti^{3+} could be accommodated in the host lattice and transformed into the Ti^{3+}–Ti^{4+} pair in the oxidation atmosphere of growth. Such a picture is consistent with the experimental fact [4,5] that a higher O_2 partial pressure during growth will lead to an increase in both IR residual absorption and UV absorptions.

In the model shown in figure 1(*b*), the two cations of the pair stacking along the *c* axis share the equilateral triangle of O atoms. Although the original site symmetry is C_3, the distortion from C_{3v} is so slight that the upper and the lower triangle, are rotated from σ_v planes by only about 2°8.5′ [14] which can be seen by the projection diagram on the plane perpendicular to the *c* axis, as shown in figure 1(*c*). Therefore the C_{3v} approximation in our computation would have little influence on the physical result.

To calculate the electronic structure of Ti^{3+}, the usual selection of the cluster model is taken as the cation with its nearest anion ligands, i.e. the cluster $(Ti^{3+}O_6^{2-})^{9-}$ for Ti^{3+} in Al_2O_3 (figure 2). The effect of the nearest cation has also been taken into consideration by some workers [8]. In our work, in order to compare with the ion pair model of Ti^{3+}–Ti^{4+}, the same pair structure of $(Ti^{3+}Al^{3+}O_9^{2-})^{12-}$ is chosen to compute the crystal-field structure of Ti^{3+} in $Ti:Al_2O_3$. Nevertheless, the calculation result with the cluster $(Ti^{3+}O_6^{2-})^{9-}$ is also presented as a comparison with that of $(Ti^{3+}Al^{3+}O_9^{2-})^{12-}$.

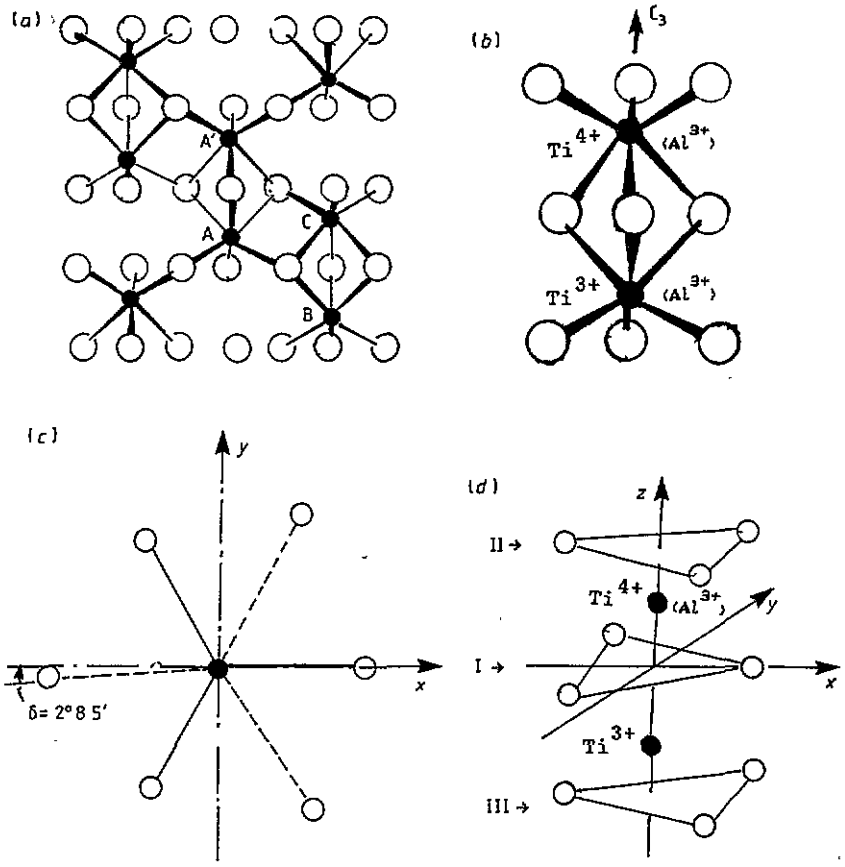

Figure 1. (*a*) Structure of α-Al_2O_3 (○: O^{2-}, ●: Al^{3+}) three type pair interaction are available: (i) A–B, Cation–Anion–Cation; (ii) A–C, Cation–Cation sharing a common edge; (iii) A–A′, Cation–Cation sharing a common face. (*b*) Pair model selected in calculation (○: O^{2-}; ●, either Ti^{3+} and Al^{3+} for $(Al^{3+}Ti^{3+}O_8^{2-})^{12-}$ or Ti^{3+} and Ti^{4+} for $(Ti^{3+}Ti^{4+}O_9^{2-})^{11-}$). (*c*) Projection of the pair model on the plane perpendicular to C_3 axis; on account of δ is very small, C_{3v} approximation is adopted. (*d*) Selection of the coordinate system.

The computation parameters selected and shown in table 1, with regard to figure 1(*d*), are taken from [14, 15]. Proper adjustment of the bonding distance is essential when a foreign ion is introduced into the host lattice. The bond length adopted here is the sum of the radii of the bonding ions, e.g. bond length $(Ti^{3+}–O^{2-}) = r(Ti^{3+}) + r(O^{2-})$, where r represents the ion radius.

The variational basis sets and the corresponding parameters of the funnel potential well (figure 3) subjected to them [8] are listed in table 2. To guarantee a plausible result, proper selection of parameters of the potential well should be made so that the result would not be very sensitive to adjustments of the parameters. In our experience, it is found that it will ease the selection if the following physical considerations are complied with.

(1) $r < R_1$, $R_2 < d$, where r is the ion radius, R_1 and R_2 are the inner and outer widths of the well confining the ion and d is the distance of the ion to its nearest-neighbour ion.

(2) The valence orbit of the cations should be tighter than that of the anion O^{2-}; hence the difference between R_1 and R_2 for the cations should be smaller than the radius of O^{2-}.

(3) The average width of the potential well of cations should be matched with their

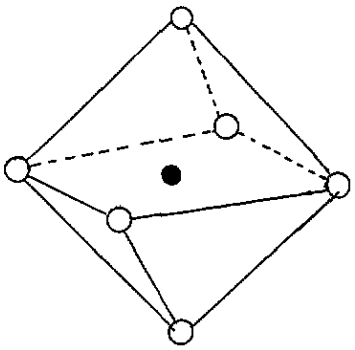

Figure 2. Cluster $(Ti^{3+}O_6^{2-})^{9-}$ with O_h symmetry.

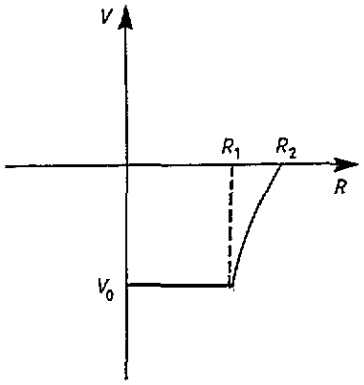

Figure 3. Funnel potential well in DV-X_α method.

Table 1. Structure parameters of the cluster $Ti^{3+}Al^{3+}O_9^{2-}$. The coordinates refer to figure 1(*d*). The subscripts I, II and III indicate the coordinates of the first ion of each symmetry type of O^{2-} under C_{3v} symmetry.

	Ti^{3+}	Al^{3+}	O_I^{2-}	O_{II}^{2-}	O_{III}^{2-}	Reference
x (au)	0.00	0.00	2.85	−3.04	−3.00	[14]
y (au)	0.00	0.00	0.00	0.00	0.00	[14]
z (au)	−2.55	2.36	0.00	4.10	−4.64	[14]
x (au)	0.00	0.00	2.96	−2.93	−3.00	[15]
y (au)	0.00	0.00	0.00	0.00	0.00	[15]
z (au)	−2.30	2.10	0.00	4.15	−4.18	[15]

Table 2. Ion basis sets and parameters for the funnel potential well.

	Ion basis sets	R_1 (au)	R_2 (au)	V_0 (au)
O^{2-}	$1s^22s^22p^63s^03p^0$	2.6	3.5	−3.0
Al^{3+}	$1s^22s^22p^63s^03p^0$	2.4	2.6	−2.0
Ti^{3+}	$1s^22s^22p^63s^23p^63d^14s^04p^0$	2.7	3.3	−2.0
Ti^{4+}	$1s^22s^22p^63s^23p^63d^04s^04p^0$	2.7	3.1	−2.0

ion radii, namely $\bar{R}(Ti^{3+}) : \bar{R}(Ti^{4+}) : \bar{R}(Al^{3+}) \simeq r(Ti^{3+}) : r(Ti^{4+}) : r(Al^{3+})$, where $\bar{R} = (R_1 + R_2)/2$.

The spin-polarized scheme is adopted in our DV-X_α calculation. All the energy values presented were obtained by the transition-state calculation. Lower-energy orbits of 1s–2p for Ti^{3+} and 1s for O^{2-} and Al^{3+} are treated as frozen cores. A charged Waston sphere is taken to enclose the cluster so as to inflict to some degree the effect of the crystal environment and to keep the system electrically neutral. The parameters of the sphere and the total number of diophantine sampling points for different clusters are listed in table 3. The convergency accuracy of the self-consistent charge process is 10^{-4}.

3. Results and discussion

The computation provides a molecular orbital population analysis which gives the

Table 3. DV-X_α calculation parameters.

Cluster	Waston sphere radius (au)	Parameter charge	Number of diophantine sample points
$(Ti^{3+}O_6^{2-})^{9-}$	5.6	+9	2100
$(Ti^{3+}Al^{3+}O_9^{2-})^{12-}$	7.5	+12	3600
$(Ti^{3+}Ti^{4+}O_9^{2-})^{11-}$	7.5	+11	3600

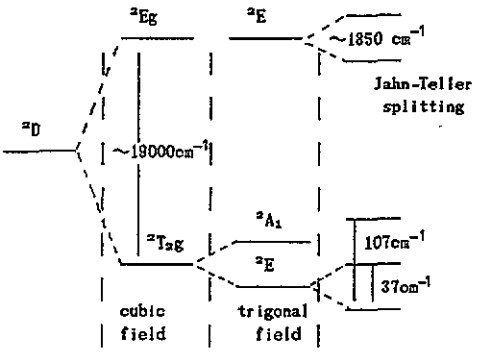

Figure 4. Crystal field structure of Ti^{3+} in Al_2O_3.

proportions of a single atomic orbit in each molecular orbit. According to this information, the energy structure of the cluster can be classified into three parts as shown in figures 5–7:

(i) non-bonding states by 1s–2p orbits of O^{2-} or Al^{3+} as well as 1s–3p orbits of either Ti^{3+} or Ti^{4+};

(ii) antibonding states by 3s, 3p orbits of O^{2-} or Al^{3+} and 4s, 4p orbits of Ti^{3+} or Ti^{4+};

(iii) 3d-dominated levels between the non-bonding and antibonding states which correspond to the crystal-field spectral transitions ($t_{2g} \rightarrow e_g$).

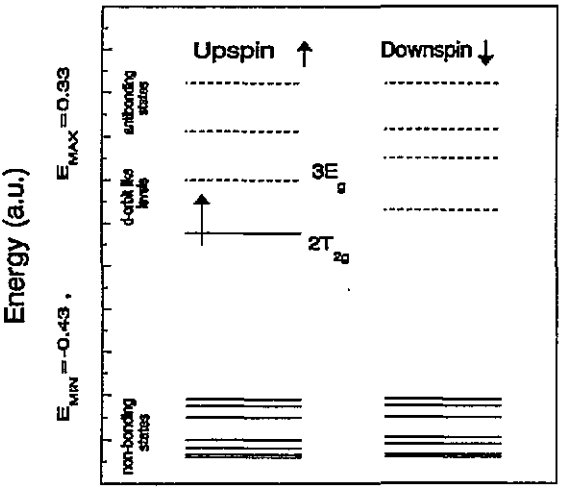

Figure 5. Energy level of cluster $(Ti^{3+}O_6^{2-})^{9-}$.

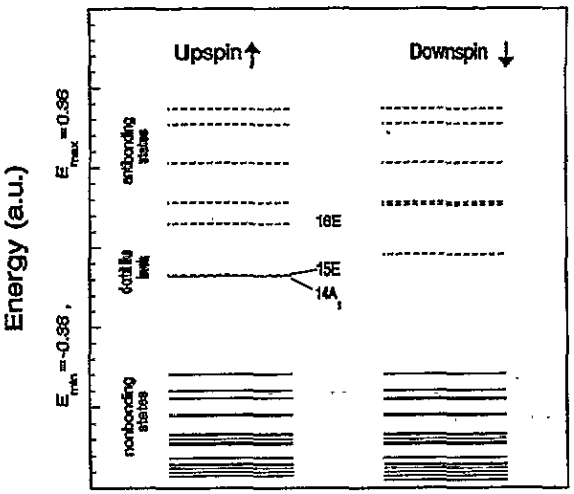

Figure 6. Levels of cluster $(Ti^{3+}Al^{3+}O_9^{2-})^{12-}$.

Table 4. Crystal-field-like energy levels and their orbital population analysis. $|Ti^{3+}:d\rangle$ indicates the d-electron contribution by Ti^{3+}; $|Ti^{4+}:d\rangle$ is the contribution by $|Ti^{4+}\rangle$; $|Al^{3+}\rangle$ is the contribution of all ionic orbitals of Al^{3+}; $|O^{2-}\rangle$ is the contribution of O^{2-}.

Cluster	Orbital type	Energy level (cm^{-1})		Orbital populations		
		Calculated	Experimental	$\|Ti^{3+}:d\rangle$	$\|Ti^{4+}:d\rangle(\|Al^{3+}\rangle)$	$\|O^{2-}\rangle$
$(TiO_6)^{9-}$	$2T_{2g}$	0	0	0.90		0.08
	$3E_g$	20490	20410	0.73		
$Al^{3+}Ti^{3+}O_9^{2-}$	$14A_1$	0		0.88	0.003	0.11
	15E	91	56	0.90	0.0005	0.10
	16E	20500	20410	0.72	0.0003	0.28
$Ti^{3+}Ti^{4+}O_9^{2-}$	$14A_1$	0		0.53	0.28	0.19
	15E	12300	12500–11760	0.86		0.13
	16E	19270	18800		0.88	0.11
	$15A_1$	22420	22026	0.32	0.56	0.12
	17E	34000	31948	0.68		0.31
	18E	39200	39416		0.71	0.28

The results as well as the corresponding experimental values are listed in table 4. The diagrams of energy levels of each model can be seen in figures 5–7.

3.1. Electronic structure of the pair model by the DV-X_α method

3.1.1. Crystal-field splitting by the model $(Ti^{3+}O_6^{2-})^{6-}$. The d electron of Ti^{3+} is split into a triplet t_{2g} and a doublet e_g under O_h symmetry and its interval distance corresponds to the CFS energy $10Dq = \Delta E(2t_{2g} \rightarrow 3e_g) = 20490\ cm^{-1}$, very close to the peak value of $20410\ cm^{-1}$ [5] in the absorption spectrum.

3.1.2. Crystal-field structure by the pair model $(Ti^{3+}Al^{3+}O_9^{2-})^{12-}$. Further splitting on some degenerate levels will take place when the actual symmetry of the clusters is taken into

consideration. For the cluster $(Ti^{3+}Al^{3+}O_9^{2-})^{12-}$ under C_{3v} symmetry, the former t_{2g} level under O_h symmetry is split into a singlet A_1 and a doublet E level. The splitting interval by our calculation is $\delta_{calc}(14A_1 \rightarrow 15E) = 91\ cm^{-1}$, which nearly fits the average value obtained from the experimental data [19], namely $\delta_{exp} = 56\ cm^{-1}$. By this model, the CFS energy $10Dq$ is 20500 cm^{-1}, corresponding to the transition $14A_1 \rightarrow 16E$.

It should be pointed out that the order of $14A_1$ and 15E, the two splitting levels of the former $2t_{2g}$ (figure 6), is reversed from that deduced by crystal-field theory [19] (figure 4) in which the A_1 level is above the doublet E level accounting for the stability of configuration. This inconsistency can be interpreted as follows. Our result is based upon the 'one-electron' approximation in which the interaction between configurations is not taken into consideration. By our method, the fully occupied ground state of A_1 will lead to a closed electronic shell for which the configuration is stable. Otherwise, if the doublet 15E were the ground state, it would lead to an open electronic shell which would be unstable and the Jahn–Teller effect would occur. Processing with this problem, however, is beyond the scope of our method.

3.1.3. Electronic structure of the Ti^{3+}–Ti^{4+} pair. Overall six crystal-field-like levels are obtained for the cluster $(Ti^{3+}Ti^{4+}O_9^{2-})^{11-}$. According to the orbital population analysis listed in table 4, the 15E and 17E levels are mainly contributed by the d orbits of Ti^{3+} and the 16E and 18E levels by the d orbits of Ti^{4+}. Although the two A_1-type orbitals, $14A_1$ and $15A_1$, could be related to Ti^{3+} and Ti^{4+}, respectively, their orbital populations also demonstrate that their d orbit contributions are mixed. This can be interpreted as the fact that the A_1-type orbital, whose wavefunction is that of d_{z^2}, is along the Z axis and the orientation of this orbital is of prime importance in the assumption of an electron cloud.

The transition from the ground state $14A_1$ to the first excited state 15E is 12300 cm^{-1}, belonging to the experimental IR residual absorption energy. The $14A_1$ and 15E levels leading to this absorption can be compared with the two splitting levels of t_{2g} of the cluster $(Ti^{3+}Al^{3+}O_9^{2-})^{12-}$. When a Ti^{3+}–Ti^{4+} pair forms with Ti^{4+} instead of the site of Al^{3+} in the cluster $(Ti^{3+}Al^{3+}O_9^{2-})^{12-}$, the more positive charge involved by Ti^{4+} will lead the energy of ground state $14A_1$ of the cluster to drop lower than that of $14A_1$ of the cluster $(Ti^{3+}Al^{3+}O_9^{2-})^{12-}$; as is demonstrated in table 4, the former splitting of t_{2g} in the Ti^{3+}–Al^{3+} model which is 91 cm^{-1} now becomes 12300 cm^{-1} in the Ti^{3+}–Ti^{4+} model. Obviously, the formation of this IR residual level can be ascribed to the influence of the Ti^{4+} ion.

The $14A_1 \rightarrow 16E$ transition of 19270 cm^{-1} is well demonstrated by the energy line in the excitation spectrum obtained by Powell *et al* [3]. Lacovara *et al* [2] observed three fluorescence bands with exciting wavelengths of 454 nm (22026 cm^{-1}), 313 nm (31948 cm^{-1}) and 253.7 nm (39416 cm^{-1}), respectively. Despite this, they associated these levels with other defects [2]; these data are well fitted by the calculated transition intervals $\Delta E(14A_1 \rightarrow 15A_1) = 22420\ cm^{-1}$, $\Delta E(14A_1 \rightarrow 17E) = 34000\ cm^{-1}$ and $\Delta E(14A_1 \rightarrow 18E) = 39200\ cm^{-1}$. Furthermore, as we mentioned in section 1, a small absorption hump at 4.5–5.0 eV, besides the broad absorption edge in the UV region, was related to iron impurities by Tippens [7], but this assignment has been questioned by later workers [2, 3, 6]. For the pair model Ti^{3+}–Ti^{4+}, the calculated transition $\Delta E(14A_1 \rightarrow 18E) = 39200\ cm^{-1}$ (4.4 eV) agrees with this absorption peak.

3.2. Charge-transfer transition

Associated with the UV absorption spectrum, the charge-transfer transition due to the 3d series TM ions in corundum has been investigated systematically by Tippens [7] using

Table 5. Charge-transfer energy.

Prediction by our calculation	Tippens' prediction	Observed data
Ti^{3+}		
8.3 eV (by $Ti^{3+}O_6^{2-}$)		
8.1 eV (by $Al^{3+}Ti^{3+}O_9^{2-}$)	7.8 eV	
Ti^{3+}–Ti^{4+}		
7.1 eV (by $Ti^{3+}Ti^{4+}O_9^{2-}$)		6.9 eV

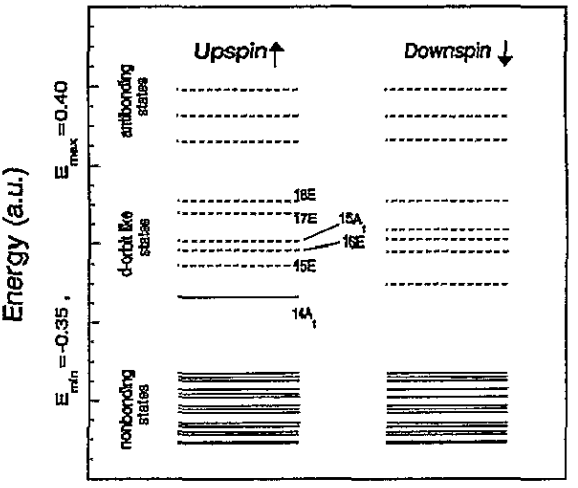

Figure 7. Levels of cluster $(Ti^{3+}Ti^{4+}O_9^{2-})^{11-}$.

molecular orbital calculations. In Tippens' data, it is surprising that the results of all other TM ions compare well with experimental data except for Ti:Al_2O_3 for which the prediction is about 1 eV larger than the observed value of 6.9 eV. Moreover, it was pointed out later by Moulton [6] that the extinction coefficient of this absorption is surprisingly smaller than that expected for Ti^{3+} and it is suggested that the absorption is in fact not due to Ti^{3+} but may be due to Ti^{4+} with regard to the work of Nath and Walda [17] and Bessonova *et al* [18].

The charge-transfer transition is a direct result of our method. According to Tippens' [7] theory, the charge-transfer transition of the d^1 electron connects an initial and a final configuration of $t_{2g}^{\uparrow}e_g$ and $t_{2g}^{\uparrow\uparrow}e_g$, respectively. Hence, the charge-transfer transition energy means the transition from the non-bonding orbits of O (2p) to the ground state of the d^1 configuration. Our result as well as Tippens' data are listed in table 5. It is seen that the transfer energy (8.1 eV) of Ti^{3+} obtained by the cluster $(Ti^{3+}Al^{3+}O_9^{2-})^{12-}$ is very close to the value of 8.3 eV obtained by the cluster $(Ti^{3+}O_6^{2-})^{6-}$ as well as to the value of 7.8 eV from Tippens' prediction. Significantly, the charge-transfer energy of the cluster $(Ti^{3+}Ti^{4+}O_9^{2-})^{11-}$ is 7.1 eV which is very close to the observed 6.9 eV UV absorption. Therefore, this clarifies Moulton's doubt about whether the observed UV absorption hump is in fact not due to the charge-transfer transition of Ti^{3+} but is due to that of the Ti^{3+}–Ti^{4+} ion pair. Hence it is not strange for the extinction coefficient of the 6.9 eV absorption to be very small because the concentration of Ti^{3+}–Ti^{4+} pairs is very small when compared with that of the predominating Ti^{3+} ion in Ti:Al_2O_3.

4. Summary

The ion pair model of Ti^{3+}–Ti^{4+} was formerly proposed to try to interpret the IR residual absorption of Ti:Al_2O_3. However, by our calculation, it is found that not only is the ion pair postulation on IR residual absorption quantitatively supported, but also the origins of the UV absorption hump and those fine absorption peaks in this region can be well explained. Additionally, as a comparison with this pair model, the crystal-field structure of Ti^{3+} is computed for the same pair structure and the crystal-field splitting value obtained also fits the experimental data well. From these results, we conclude that the Ti^{3+}–Ti^{4+} ion pair is an important local structure in the laser crystal Ti:Al_2O_3.

Acknowledgments

The work was supported by the National Science Foundation of China. The computation was completed on the VAX8700 computer at the Computation Center of Univeristy of Science and Technology of China. The authors are grateful to Dr Chuan-Yun Xiao and Dr Bi-Cai Pan for their help during this work. The analysis of some of the results was enlightened by discussion with Dr Jin-Long Yang.

References

[1] Moulton P F 1985 *Tunable Solid Lasers (Springer Series in Optical Science 47)* ed P Hammerling *et al* (Berlin: Springer) p 4
[2] Lacovara P, Esterowitz L and Kokta M 1985 *IEEE J. Quantum Electron.* **QE-21** 1614
[3] Powell R C, Caslavsky J L, Al Shaleb Z and Bowen J M 1985 *J. Appl. Phys.* **58** 2331
[4] Aggarwal R L, Sanchez A, Stuppi M, Fahey R E, Strauss A J, Rapoport W R and Khattak P 1988 *IEEE J. Quantum Electron.* **QE-24** 1003
[5] Sancehz A, Strauss A J, Aggarwal R L and Fahey R E 1988 *IEEE J. Quantum Electron.* **QE-24** 995
[6] Moulton P F 1986 *J. Opt. Soc. Am.* B **3** 125
[7] Tippens H H 1970 *Phys. Rev.* B **1** 1263
[8] Xia S D, Guo C X, Lin L B and Ellis D E 1987 *Phys. Rev.* B **35** 7671
[9] Xiao C Y, Yang J L, Xia S D and Wang K L 1992 *J. Phys.: Condens. Matter* **4** 5181
[10] Ellis D E and Painter G S 1970 *Phys. Rev.* B **2** 2887
[11] Ellis D E, Benesh G A and Byrom E 1979 *Phys. Rev.* B **20** 1198
[12] Ellis D E, Guenzburger D and Jansen H B 1983 *Phys. Rev.* B **28** 3697
[13] Goodenough J B 1960 *Phys. Rev.* **117** 1442
[14] MacClure D S 1962 *J. Chem. Phys.* **36** 2757
[15] Batra I P 1982 *J. Phys. C: Solid State Phys.* **15** 5899
[16] Abrahams S C 1963 *Phys. Rev.* **130** 2230
[17] Nath G and Walda G 1968 *Z. Naturf.* a **28** 624
[18] Bessonova T S, Stanislavskii M P and Khaimov Malkov V Y 1976 *Opt. Spectrosc. (USSR)* **41** 87
[19] Nelson E D, Wong J Y and Schalow A L 1967 *Phys. Rev.* **156** 298